Deep Learning-Based Displacement Tracking for Post-Stroke Myofascial Shear Strain Quantification

Md Ashikuzzaman[1], Jonny Huang[2], Steve Bonwit[2], Azin Etemadimanesh[2], Preeti Raghavan[2], and Muyinatu A. Lediju Bell[1,3,4]

[1]Department of Electrical and Computer Engineering, Johns Hopkins University, Baltimore, MD, USA
[2]Department of Physical Medicine and Rehabilitation, Johns Hopkins Medicine, Baltimore, MD, USA
[3]Department of Biomedical Engineering, Johns Hopkins University, Baltimore, MD, USA
[4]Department of Computer Science, Johns Hopkins University, Baltimore, MD, USA

***Abstract*—Shear strain measurements derived from ultrasound imaging of tissue displacements have the potential to be a useful biomarker of muscle health, myofascial stiffness, and associated pain. However, displacement tracking techniques that were previously implemented to discern this potential are limited by displacement estimation noise and lengthy runtimes. This work investigates the ability of a deep learning-based displacement tracking method applied to myofascial shear strain quantification to resolve these two limitations. A pre-trained recurrent all-pairs field transforms (RAFT) network was deployed on *in vivo* shoulder muscle data acquired from two stroke patients. Results were compared to a conventional window-based tracking approach. RAFT reduced the estimation variance by factors of 354-667 relative to the conventional approach, which manifests as smoother lateral displacement images. When each post-displaced image was warped by the estimated displacement, RAFT reduced the maximum residual between the pre- and post-displaced images by 19-23%, when compared to the conventional approach. In addition, RAFT completed displacement tracking of consecutive image pairs in 0.25 seconds, which is one of the greatest advantages of RAFT for the proposed clinical application. Results are promising to quantify myofascial stiffness and monitor muscle health with real-time speed (e.g., 4 Hz).**

***Index Terms*—Ultrasound, shear strain, displacement tracking, deep learning, stroke, myofascial stiffness**

I. INTRODUCTION

Shear strain properties have traditionally served as biomarkers of tissue pathologies (e.g., tumor malignancy, cardiovascular abnormality) [1]–[3]. Recent investigations have also supported a novel clinical hypothesis that the pectoralis muscles on the post-stroke paretic side of a patient dysfunctionally glide against fascial layers, causing increased myofascial pain and stiffness relative to the non-paretic side [4]. These physiological effects are further hypothesized to be responsible for alterations in the lateral shear strain between the pectoralis major and minor muscles on the paretic and non-paretic sides after a stroke [5]–[7].

Fundamentally, ultrasonic shear strain estimation requires tracking the displacement fields between images, then differentiating the associated displacement component (e.g., axial, lateral) with respect to an orthogonal spatial direction. Therefore, displacement estimation is arguably the most critical component of the shear strain quantification process, because shear strain accuracy is directly related to the quality of the estimated displacements. Window-based [8] and energy function optimization-based [9]–[11] techniques are two of the most traditional ultrasonic displacement estimation methods. Previous work utilized window-based [6], [7], [12] tracking to quantify myofascial shear strain. However, window-based techniques are sensitive to speckle-tracking noise. In addition, both window-based and energy-based techniques require an exhaustive search process, which can limit real-time implementation and investigations.

Deep learning-based tracking is an emerging approach that has the potential to overcome the noise and/or real-time implementation limitations of window- and energy-based algorithms [13]–[15]. In particular, deep learning models can produce accurate, low-variance displacement fields with inference rates of 11 Hz [14], which is suitable for real-time implementation. While energy-based techniques can also address the noise limitation of window-based techniques [5], this approach remains limited by slow implementation speeds (e.g., 0.2 Hz [11]). Therefore, deep learning-based tracking has the potential to both reduce noise and increase implementation speed with respect to quantifying myofascial shear strain in stroke patients.

This paper investigates the feasibility of deep learning-based ultrasound displacement tracking of myofascial shear strains. In particular, a deep optical flow estimation network, named recurrent all-pairs field transforms (RAFT) [16], is deployed to track myofascial shear strain in patients with post-stroke shoulder pain. We compare deep learning to standard window-based tracking techniques, as the majority of existing myofascial shear strain quantification research employs window-based techniques [6], [7], [12].

II. METHODS

A. *In Vivo* Data Acquisition

A bimanual arm trainer (Mirrored Motion Works Inc., Raleigh, NC) was utilized to passively rotate the shoulders of two research participants with stroke, each with one painful paretic shoulder. The shoulders were periodically rotated internally (0-30° excursion) at a rate of 0.5 Hz. A robot-held L15 ultrasound probe (Clarius Moblie Health, Vancouver, BC) was placed to acquire 20 seconds of envelope-detected ultrasound data from the pectoralis muscles of each participant during the passive motion described above. The ultrasound

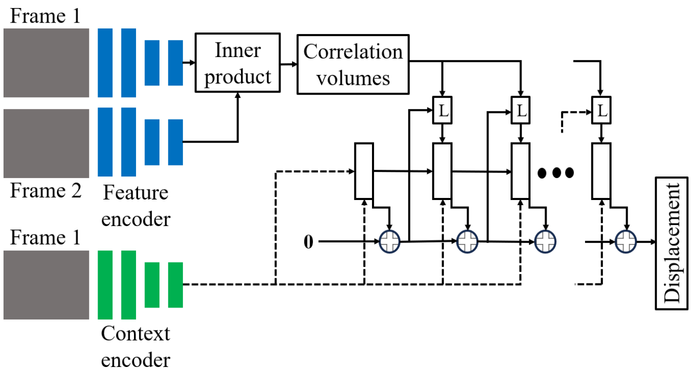

Fig. 1: RAFT architecture

transmit and sampling frequencies were 14 MHz and 15 MHz, respectively. This research study was approved by the Johns Hopkins Institutional Review Board, and patients provided written consent to participate.

B. Displacement Tracking

RAFT [16] was implemented in PyTorch [17] to perform the previously unseen task of tracking tissue displacements between consecutive ultrasound frames, according to the network architecture shown in Fig. 1. This architecture accepts pre- and post-displaced image acquisitions (i.e., Frames 1 and 2, respectively) as inputs to two convolutional neural networks with the same architecture, which calculates the inner products between extracted features to construct a correlation volume, then iteratively estimates displacement fields. A single calculation of context features from Frame 1 is also provided using the same network architecture as that of the feature encoder. Initialized with zero displacement values, RAFT updates the displacement estimates using a modified gated recurrent unit [18] in each iteration. The input to the update block is a combination of context features and correlation and displacement features, respectively, extracted from the correlation volume and the current displacement estimates. This process was repeated for each ultrasound frame pair (totaling 473 and 418 for Participants 1 and 2, respectively).

We tested a pre-trained RAFT model on our ultrasound dataset. Pre-training was implemented with FlyingChairs [19] + FlyingThings3D [20] datasets, followed by fine-tuning on the Sintel [21] dataset. The supervised loss function was defined as:

$$Loss = \sum_{i=1}^{N} w^{N-i} \|\mathbf{d}_g - \mathbf{d}_i\|_1 \tag{1}$$

where N is the number of iterations, $\mathbf{d}_g$ and $\mathbf{d}_i$ refer to the ground truth and estimated displacement fields, respectively, and w is a tunable weight, empirically set to 0.8. More details are available in [16].

Each input frame pair illustrated in Fig. 1 was envelope-detected ultrasound data, normalized to [-1 1], and resized to 520×960. The displacement estimates were then resized back to the original size of the input frames with appropriate scaling of the displacement values.

C. Quantitative Assessments

For each frame pair, the pixel-wise displacement difference between Frames 1 and 2 (after warping Frame 2 by the estimated displacement field) was calculated, which is referred to as the residual. To assess displacement tracking accuracy, the maximum absolute residual (MAR) was calculated, with lower values indicating greater accuracy. To assess the variability of the displacement estimates, the variance (σ) within a 5 mm $\times$ 5 mm spatial window of each lateral displacement image was calculated.

To connect displacement measurements to the clinical hypothesis of myofascial shear strain and stiffness differences between paretic and non-paretic shoulders, lateral displacement estimates between consecutive frames were temporally accumulated. The instantaneous shear strains were calculated using the cumulative lateral displacement estimates:

$$\text{Shear strain} = \frac{l_{\text{c,minor}} - l_{\text{c,major}}}{D} \times 100\% \tag{2}$$

where $l_{\text{c,major}}$ and $l_{\text{c,minor}}$ denote the average cumulative lateral displacements within 5 mm $\times$ 5 mm rectangular regions of interest (ROIs) placed on the pectoralis major and minor muscles, respectively, and D is the axial distance between the ROI centers. The calculated shear strains were then plotted as a function of time, and the median of each plot was reported.

The above process was repeated with a cross-correlation-based windowed-search technique [8] (hereafter referred to as Search). The MAR, σ, and shear strain results obtained with Search were compared to those produced with RAFT. In addition, the execution times to perform Search and RAFT were also compared.

III. Results

Fig. 2 shows representative single-frame B-mode images and corresponding lateral displacement images produced by Search and RAFT. Both approaches successfully delineate the primary motion directions of the pectoralis major and minor muscles. However, Search produces characteristic displacement estimation noise that is inconsistent with the controlled passive shoulder motion (σ values of 0.052 and 0.24 mm^2 for Participants 1 and 2, respectively). This noise was reduced with RAFT, resulting in σ values of 7.86×10^{-6} and 3.63×10^{-5} mm^2 for Participants 1 and 2, respectively. Across the entire 473 (Participant 1) and 418 (Participant 2) frame pairs, Table I shows that RAFT reduced σ by factors of 354-667 and also reduced the MAR by 19-23% per participant, when compared to corresponding Search results. These reductions are achieved despite discrepancies with the shear plane contour in the example RAFT results (Fig. 2).

Figs. 3(a) and 3(b) present the progression of lateral shear strain over time for Participants 1 and 2, respectively. RAFT generally produces smoother shear strain profiles than Search. In particular, whereas abrupt jumps exist with Search (which

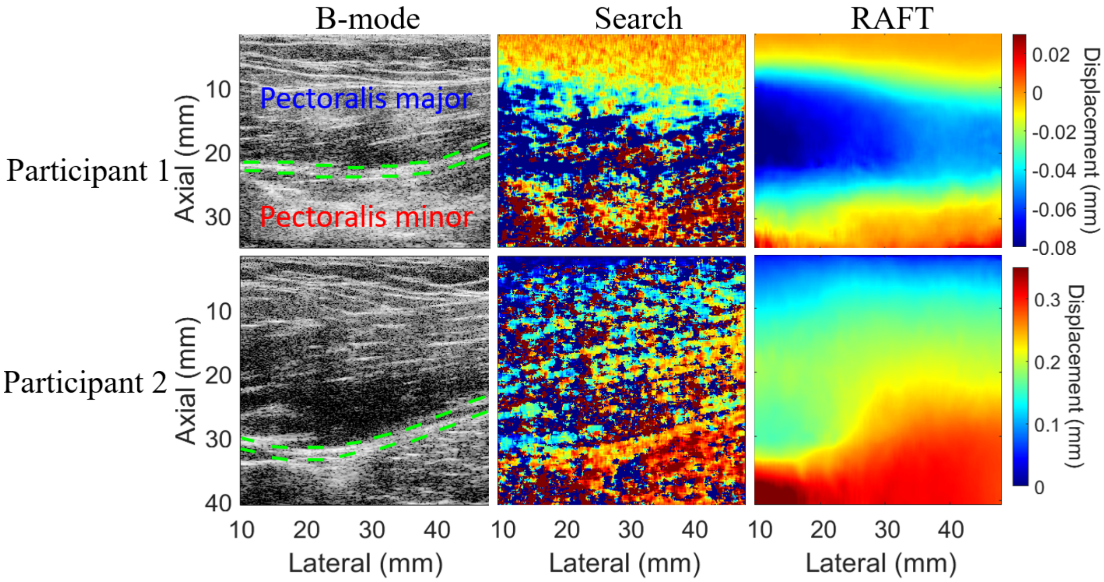

Fig. 2: Representative B-mode and lateral displacement images from the non-paretic side of the two participants. The dashed lines in the B-mode images indicate the myofascial shear plane.

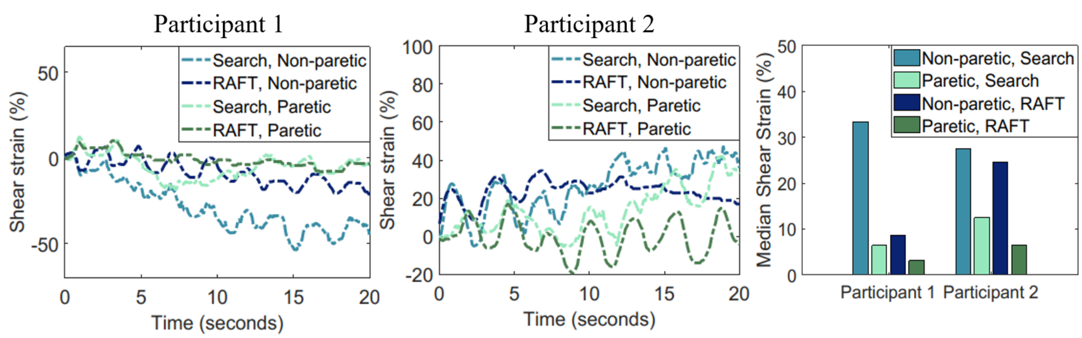

(a) (b) (c)

Fig. 3: Quantitative shear strain as a function of time for Participants (a) 1 and (b) 2. (c) Median shear strains obtained from the plots in (a) and (b).

are unexpected based on the controlled data acquisition protocol), RAFT provides nearly flat or more cyclical strain patterns for each participant.

Fig. 3(c) shows the corresponding median shear strain summary (i.e., median shear strain of each plot in Figs. 3(a) and 3(b)). Based on these results, the paretic side of each patient experiences lower lateral shear than the non-paretic side. In particular, for Participants 1 and 2, the non-paretic to paretic median shear strain ratios are 5 and 2, respectively, with Search and 3 and 4, respectively, with RAFT.

TABLE I: Mean $\pm$ standard deviation of MAR and σ measurements. Bold indicates best per metric per participant.

Participant		MAR (mm)	σ (mm^2)
1	Search	0.74 ± 0.09	0.20 ± 0.13
	RAFT	$\mathbf{0.60 \pm 0.10}$	$\mathbf{0.00030 \pm 0.0014}$
2	Search	0.80 ± 0.07	0.29 ± 0.15
	RAFT	$\mathbf{0.62 \pm 0.10}$	$\mathbf{0.00082 \pm 0.0035}$

With an NVIDIA TITAN Xp GPU with 27.9 GB memory, RAFT required approximately 0.25 s to estimate the displacements between two consecutive 36.2 mm $\times$ 49.92 mm ultrasound images (1 minute to process the entire video acquisition from the non-paretic side of Participant 1, which contains 240 frames total). In comparison, with a 6th generation Intel Core-i5 CPU with 32 GB RAM, Search required approximately 29 seconds to estimate the displacement fields between the same two frames noted above (116 minutes to process the entire video acquisition containing 240 frames).

IV. Discussion

This study is the first to demonstrate a deep-learning-based displacement tracking approach to determine post-stroke myofascial shear strain. RAFT is an otherwise established optical flow approach for natural images and photographs that, to the best of our knowledge, has never been implemented for this new clinical task. The benefits of RAFT-based myofascial shear strain estimation include qualitatively interpretable displacement images and shear strain trajectories, quantitative improvements over a more standard approach (Table I), and real-time runtimes. In addition, the proposed deep learning approach supports the clinical hypothesis that the paretic side of a stroke patient yields lower shear strain than the non-paretic side (Fig. 3(c)).

RAFT provided displacement estimates with a factor of 116 times lower runtime than Search. Whereas Search was implemented on a CPU, RAFT was implemented on a GPU, which can be considered as an unfair runtime comparison, particularly if the runtime of Search can be improved with a GPU-optimized algorithm. However, previous work [22] reports a window-based displacement tracking algorithm runtime of 3 s when implemented on a GPU to produce a 50 pixels $\times$ 300 pixels displacement image. This speed is slower than the 0.25 s runtime achieved with our deep learning-based tracking approach, which also produced a larger 520 pixels $\times$ 960 pixels displacement image. Therefore, it is unlikely that a window-based tracking algorithm will outperform the speed of a deep learning approach, even if both are implemented and optimized on the same GPU.

One limitation of our study is the pre-training of RAFT on synthetic computer vision datasets to perform ultrasound motion tracking. However, it is nonetheless promising that RAFT outperformed a standard window-based tracking approach (as reported in Table I). Future work will implement unsupervised training on ultrasound videos containing primarily lateral motion to assess the potential for additional performance improvements.

V. CONCLUSION

We investigated the feasibility of a deep learning-based displacement tracking model (i.e., RAFT) to quantify post-stroke myofascial shear strain. RAFT completed this task in 0.25 s per frame pair (i.e., 4 Hz inference speed), with reduced displacement estimation variance and better accuracy relative to a window-based displacement tracking technique. In addition, RAFT generally provided smoother shear strain profiles, which enables reliable qualitative assessment of myofascial stiffness. From a clinical perspective, it is also highly promising that the presented RAFT implementation supports the hypothesis of lower lateral shear strain between the pectoralis major and minor muscles on the paretic side of stroke patients, relative to the non-paretic side, highlighting potential utility as an ultrasound biomarker of post-stroke shoulder pain.

ACKNOWLEDGMENT

This work is supported by NIH Award Numbers R61-AT012279 and R01-EB032960.

REFERENCES

[1] A. Thitaikumar *et al.*, "Breast tumor classification using axial shear strain elastography: A feasibility study," *Physics in Medicine and Biology*, vol. 53, no. 17, p. 4809, 2008.

[2] S. Nottin *et al.*, "Alteration in left ventricular normal and shear strains evaluated by 2D-strain echocardiography in the athlete's heart," *The Journal of Physiology*, vol. 586, no. 19, pp. 4721–4733, 2008.

[3] J. R. Doherty *et al.*, "Acoustic radiation force elasticity imaging in diagnostic ultrasound," *IEEE Transactions on Ultrasonics, Ferroelectrics, and Frequency Control*, vol. 60, no. 4, pp. 685–701, 2013.

[4] P. Raghavan, A. Gordon, R. Roemmich, and A. Stecco, "Treatment of focal muscle stiffness with hyaluronidase injections," in *Spasticity and Muscle Stiffness: Restoring Form and Function*, 2022, pp. 263–286.

[5] M. Ashikuzzaman, J. Huang, S. Bonwit, A. Etemadimanesh, P. Raghavan, and M. A. L. Bell, "Displacement tracking reliability in muscle shear strain quantification," in *SPIE Medical Imaging 2024*, accepted.

[6] P. Raghavan, M. Ashikuzzaman, E. Mondragon, J. Huang, L. Zhao, S. Bonwit, A. Etemadimanesh, and M. A. L. Bell, "Quantifying myofascial shear strain in chronic post-stroke shoulder pain with ultrasound shear strain measurements," in *2023 Neuroscience Meeting Planner, Program No. 409.03*. Washington, DC: Society for Neuroscience. Online, 2023.

[7] L. Zhao, J. Huang, M. A. L. Bell, and P. Raghavan, "Measuring myofascial shear strain in chronic shoulder pain with ultrasound shear strain imaging: A case report," *BMC Musculoskeletal Disorders*, in review.

[8] M. A. Lediju, M. J. Pihl, S. J. Hsu, J. J. Dahl, C. M. Gallippi, and G. E. Trahey, "A motion-based approach to abdominal clutter reduction," *IEEE Transactions on Ultrasonics, Ferroelectrics, and Frequency Control*, vol. 56, no. 11, pp. 2437–2449, 2009.

[9] M. Ashikuzzaman, A. K. Tehrani, and H. Rivaz, "Exploiting mechanics-based priors for lateral displacement estimation in ultrasound elastography," *IEEE Transactions on Medical Imaging*, vol. 42, no. 11, pp. 3307–3322, 2023.

[10] M. Ashikuzzaman, T. J. Hall, and H. Rivaz, "Incorporating gradient similarity for robust time delay estimation in ultrasound elastography," *IEEE Transactions on Ultrasonics, Ferroelectrics, and Frequency Control*, vol. 69, no. 5, pp. 1738–1750, 2022.

[11] M. Ashikuzzaman and H. Rivaz, "Second-order ultrasound elastography with $l1$-norm spatial regularization," *IEEE Transactions on Ultrasonics, Ferroelectrics, and Frequency Control*, vol. 69, no. 3, pp. 1008–1019, 2022.

[12] H. M. Langevin *et al.*, "Reduced thoracolumbar fascia shear strain in human chronic low back pain," *BMC Musculoskeletal Disorders*, vol. 12, pp. 1–11, 2011.

[13] A. K. Tehrani and H. Rivaz, "Displacement estimation in ultrasound elastography using pyramidal convolutional neural network," *IEEE Transactions on Ultrasonics, Ferroelectrics, and Frequency Control*, vol. 67, no. 12, pp. 2629–2639, 2020.

[14] S. Wen *et al.*, "Convolutional neural network-based speckle tracking for ultrasound strain elastography: An unsupervised learning approach," *IEEE Transactions on Ultrasonics, Ferroelectrics, and Frequency Control*, 2023.

[15] A. K. Z. Tehrani, M. Ashikuzzaman, and H. Rivaz, "Lateral strain imaging using self-supervised and physically inspired constraints in unsupervised regularized elastography," *IEEE Transactions on Medical Imaging*, vol. 42, no. 5, pp. 1462–1471, 2023.

[16] Z. Teed and J. Deng, "RAFT: Recurrent all-pairs field transforms for optical flow," in *Computer Vision–ECCV 2020: 16th European Conference, Glasgow, UK, August 23–28, 2020, Proceedings, Part II 16*, 2020, pp. 402–419.

[17] A. Paszke *et al.*, "Pytorch: An imperative style, high-performance deep learning library," *Advances in Neural Information Processing Systems*, vol. 32, 2019.

[18] K. Cho *et al.*, "Learning phrase representations using rnn encoder-decoder for statistical machine translation," *arXiv Preprint arXiv:1406.1078*, 2014.

[19] A. Dosovitskiy *et al.*, "FlowNet: Learning optical flow with convolutional networks," in *Proceedings of the IEEE International Conference on Computer Vision*, 2015, pp. 2758–2766.

[20] N. Mayer *et al.*, "A large dataset to train convolutional networks for disparity, optical flow, and scene flow estimation," in *Proceedings of the IEEE Conference on Computer Vision and Pattern Recognition*, 2016, pp. 4040–4048.

[21] D. J. Butler *et al.*, "A naturalistic open source movie for optical flow evaluation," in *Computer Vision–ECCV 2012: 12th European Conference on Computer Vision*, 2012, pp. 611–625.

[22] B. Peng and L. Huang, "GPU-accelerated sub-sample displacement estimation method for real-time ultrasound elastography," *Opto-Electronic Engineering*, vol. 43, no. 6, pp. 83–88, 2016.